Modeling Nonlinear Distortion of Ultra Wideband Signals at X-Band

Sonali Luniya, *Student Member, IEEE*, Kevin G. Gard, *Member, IEEE*, and Michael B. Steer, *Fellow, IEEE*

***Abstract*—Nonlinear distortion in the adjacent channels of an X-band amplifier driven by an ultra-wideband digitally-modulated carrier is analyzed. Statistical properties of the input signal with a complex power series-based behavioral model of the amplifier are used to calculate the output power spectrum. Comparisons are made between measured and predicted adjacent channel power rejection for the X-band monolithic microwave integrated circuit.**

***Index Terms*—Bandpass nonlinearity, nonlinear distortion, spectral regrowth, ultra-wideband (UWB).**

I. Introduction

In THE U.S., an ultra-wideband (UWB) system is defined as any wireless transmission scheme that occupies a fractional bandwidth of greater than 20% or more than 500 MHz of absolute bandwidth. The modified version of the Part 15.209 rules [1] permits the unlicensed deployment of ultra-wideband applications in the 3.1–10.6 GHz band, overlaying the existing licensed systems. The rules specifically limit the power spectral density to −41.2 dBm measured in 1-MHz bandwidths, i.e., a maximum transmitted power of −2.52 dBm at the output of an isotropic antenna. The regulations subject UWB devices to strictly limited transmit power requirements and stringent limits on intermodulation levels in the adjacent channels since they share the band with existing licensed wireless systems. In summary, UWB communication is allowed at a very low average transmit power compared to conventional "narrowband" systems. UWB communication systems compensate for the limited transmit power by using digitally-modulated signals with various wideband encoding schemes including direct sequence spread spectrum (DSSS) [2], orthogonal frequency division multiplexing (OFDM) [3], and direct pulse transmission. The purpose of this letter is to investigate, and present a technique for investigating, the impact of circuit- and signal-dependent distortion by examining an X-band monolithic microwave integrated circuit (MMIC) low noise amplifier. The stringent FCC requirements require that distortion in adjacent channels of a UWB system be characterized with high fidelity.

Distortion of digitally-modulated communication front-end circuits is dependent on the amplitude variation characteristics of the input signal and the nonlinear input/output characteristics of the circuits. This nonlinear distortion degrades the signal-to-noise ratio (SNR) of the transmitted signal. This in turn reduces system throughput as the transmission and modulation schemes require particularly high SNR to maintain low bit error rates (BER). Therefore, it is important to assess the amount of distortion generated by different UWB signals applied to different nonlinear wireless circuits.

The wideband nature of UWB signals presents a challenge for the evaluation of nonlinear distortion. Direct simulation of circuits and systems with UWB digital modulation requires high sampling frequencies to capture the bandwidth of the signal and distortion. What exacerbates the modeling problem is that the time-span required for simulation depends on the amount of data required to make a meaningful measurement and this can be excessive if a direct simulation technique is to be used. Behavioral modeling of high-frequency circuits simplifies computational requirements by reducing both the complexity of the model and by only computing the distortion terms of interest about the carrier frequency.

This letter analyzes the nonlinear distortion generated when a 1.2-GHz-wide BPSK signal with a center frequency of 10 GHz is applied to an X-band MMIC amplifier. Here, the amplifier is modeled from measured AM–AM AM–PM data at 10 GHz. A complex power series envelope behavioral model is then developed from this measured data and used in conjunction with a statistical analysis method to predict the spectral regrowth generated during amplification. Predicted distortion is in excellent agreement with measured results at 10 GHz. These results demonstrate that complex power series envelope behavioral models are viable technologies for accurately predicting the signal- and circuit-dependent distortion in UWB systems.

II. Nonlinear Distortion Analysis

The response of a memoryless or quasi-static nonlinearity can be accurately modeled using the AM–AM and AM–PM characteristics of the device. This assumption holds for wideband devices if the broadband nonlinear response of the device is not frequency dependent. In this case, the nonlinear response of the modulation envelope of the carrier can be described in terms of a power series description of the nonlinear response and the complex envelope of the carrier [4]

$$\tilde{G}_{\omega_c}[\tilde{z}(t)] = \sum_{n=0}^{\frac{N-1}{2}} \frac{\tilde{a}_{2n+1}}{2^{2n}} \binom{2n+1}{n+1} \tilde{z}(t)^{n+1} [\tilde{z}^*(t)]^n \qquad (1)$$

where a_n are complex power series coefficients representing a quasistatic nonlinearity and $z(t)$ is the complex envelope of the modulated carrier signal. The power spectrum of the envelope

Manuscript received December 8, 2005; revised March 7, 2006. This work was supported in part by the U.S. Army Research Office as a Multidisciplinary University Research Initiative on Multifunctional Adaptive Radio Radar and Sensors under Grant DAAD19-01-1-04 and by the William J. Pratt Assistant Professorship.

The authors are with the Electrical and Computer Engineering Department, North Carolina State University, Raleigh, NC 27695-7914 USA (e-mail: kevin_gard@ncsu.edu).

Digital Object Identifier 10.1109/LMWC.2006.875588

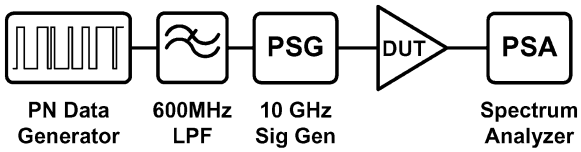

Fig. 1. Ultra wideband spectral regrowth measurement.

at the carrier frequency is obtained by computing the Fourier transform of the autocorrelation function of the carrier envelope

$$\widetilde{S}_{gg}(f) = \sum_{n=0}^{\frac{N-1}{2}} \sum_{m=0}^{\frac{N-1}{2}} \frac{\widetilde{a}_{2n+1}\widetilde{a}^{*}_{2m+1}}{2^{2(n+m)}} \binom{2n+1}{n+1} \times \binom{2m+1}{m+1} \widetilde{S}_{(2n+1)(2m+1)}(f) \quad (2)$$

where

$$\tilde{S}_{(2n+1)(2m+1)}(f) = \int_{-\infty}^{\infty} \tilde{\Re}_{z_{2n+1}z_{2m+1}}(\tau) e^{-j\omega\tau} d\tau \quad (3)$$

and

$$\tilde{\Re}_{z_{2n+1}z_{2m+1}}(\tau) = \lim_{T\to\infty} \frac{1}{2T} \int_{-T}^{T} z_1^{n+1} (z_1^*)^n z_2^m (z_2^*)^{m+1} dt. \quad (4)$$

where

$$z_1 = z(t), \quad z_2 = z(t+\tau). \quad (5)$$

The autocorrelation and spectral terms from (4) and (2) are calculated ahead of time using a realization of the UWB signal while the power series coefficients are obtained by fitting the coefficients to the AM–AM and AM–PM characteristics of the circuit.

III. Measurement Results

Generation of UWB signals is a challenge due to the expense of wideband analog to digital converters needed to create test signals. Alternatively, an UWB signal can be readily generated using a high-speed digital signal generator and a low pass filter to suppress the higher sidelobes of the data power spectrum. A 1.2-GHz-wide BPSK test signal was generated by passing a 1.2-Gb/s pseudorandom (PN) bit sequence through a 600-MHz lowpass filter. This wideband baseband signal was then applied to the modulator inputs of a vector signal generator where it was upconverted to a 10-GHz center frequency. This upconverted signal results in a UWB signal occupying 1.2 GHz of bandwidth about the carrier frequency. A block diagram of the test setup is shown in Fig. 1.

The device under test (DUT) was a high dynamic range, broadband, two-stage X-band (8.5 GHz to 14 GHz) low noise PHEMT amplifier (LMA411 from Filtronic). The class-A amplifier is reactively matched at the input and output ports and has a nominal gain of 18 dB with an power output of +17 dBm at 1-dB gain compression. The amplifier is used as a pre-driver in phased array radar applications, as a photonics

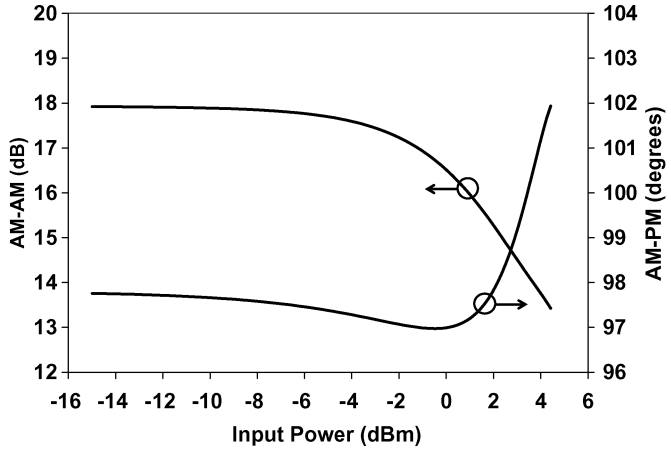

Fig. 2. Measured AM–AM and AM–PM of the X-band amplifier.

TABLE I
Coefficients of the Complex Power Series to Model the Nonlinear Device

	Real	Imaginary
$\tilde{a}_1$	-1.07003E+00	7.80747E+00
$\tilde{a}_3$	2.28416E+00	-2.16753E+00
$\tilde{a}_5$	1.92825E+01	-1.54916E+02
$\tilde{a}_7$	-2.06131E+02	6.95649E+02
$\tilde{a}_9$	4.02398E+02	-9.37203E+02

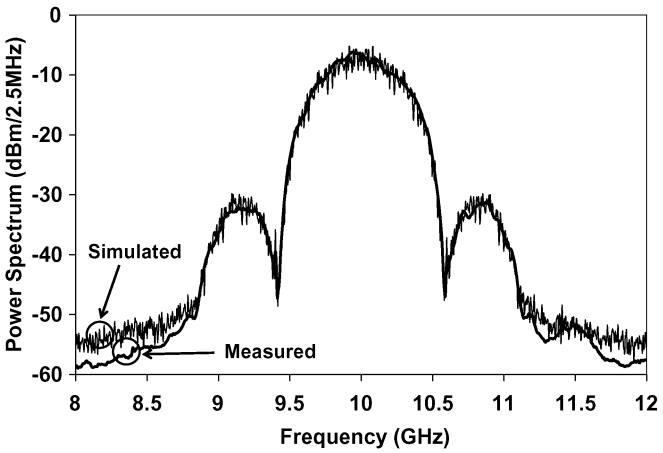

Fig. 3. Measured and simulated output power spectrum for 0-dBm input power.

predriver, and in commercial communications applications. The AM–AM and AM–PM characteristics of the amplifier, shown in Fig. 2, were measured using a vector network analyzer with an in-built power sweep function. The input power was swept from −10 dBm to 5 dBm. A complex power series behavioral model of the amplifier was generated by a least squares fit to a rectangular representation of the measurement data to a series of odd order $N = 9$ (see Table I).

The output distortion was measured using a spectrum analyzer. A comparison between the measured output power spectrum with that calculated by (2), the autocorrelation analysis approach, is shown in Fig. 3. A simulation is simple to perform and requires less than 100 ms for the signals considered

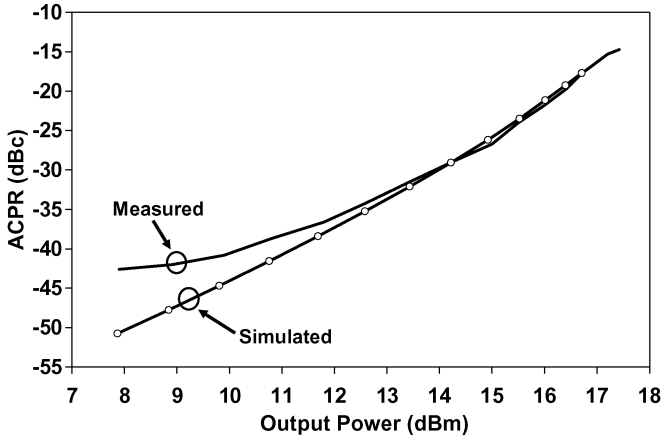

Fig. 4. Measured and predicted ACPR versus output power.

here. Simulation is in-part speeded up through precalculation of the signal statistics. As expected, distortion appearing in adjacent channels increases with larger input power levels. The level of distortion is captured by the adjacent channel power ratio (ACPR) which here is the ratio of the power in the main channel to the total power in either the upper or lower channels. The ACPR of the device was measured with a 100-MHz bandwidth at offsets of ± 800 MHz. The measured and predicted ACPR using the autocorrelation approach are shown in Fig. 4. The predicted and measured ACPR are in excellent agreement above the output power level of 13 dBm. At low input powers the measured ACPR flattens out due to the finite rejection characteristic of the lowpass filter used in generating the signal. The impact of finite filter rejection was not captured in the simulation.

The simulated spectral analysis of (2) was performed by first calculating the 16 spectral terms for an $N = 9$ odd order power series behavioral model. Each spectral term is calculated from autocorrelation estimates (4) of the BPSK input signal modulation. The estimated spectral terms are saved to a file and used at runtime to calculate the output power spectrum. The power spectrum calculation from (2) is simply a weighting of each spectral term by the input power and the pair of power series coefficients. Calculations swept over input power are very fast taking less than 100 ms for the simulated results shown in Fig. 4. In the 8–9 GHz range the simulated spectrum is higher than the measured because the simulations use sampled measurements of the filtered input signal. The noise floor of the simulation input signal is limited by the dynamic range of the sampling oscilloscope used to characterize the filtered baseband signal.

IV. Conclusion

Spectral regrowth of a 1.2-GHz-wide BPSK UWB X-band signal applied to an X-band amplifier was accurately predicted. This work demonstrated two things. One is that an AM–AM and AM–PM model (implemented here in a complex power series behavioral model) can reliably be used to determine the performance of an X-band amplifier with negligible memory-effect. The second is that an efficient statistical analysis technique is able to capture nonlinear distortion of an ultra-wideband signal.

Acknowledgment

The authors wish to thank the K. M. Gharaibeh for his assistance in running spectral regrowth simulations.

References

[1] FCC, "Revision of Part 15 of the Commission's Rules Regarding Ultra-Wideband Transmission Systems," Tech. Rep. ET-Docket 98-153, Washington, DC, Apr. 2002.

[2] P. Runkle, J. McCorkle, T. Miller, and M. Welborn, "DS-CDMA: the modulation technology of choice for UWB communications," in *Proc. IEEE Conf. Ultra Wideband Syst. Technol.*, Nov. 16–19, 2003, pp. 364–368.

[3] S. Roy, J. R. Foerster, V. S. Somayazulu, and D. G. Leeper, "Ultrawideband radio design: the promise of high-speed, short-range wireless connectivity," *Proc. IEEE*, vol. 92, no. 2, pp. 295–311, Feb. 2004.

[4] K. G. Gard, L. E. Larson, and M. B. Steer, "The impact of RF front-end characteristics on the spectral regrowth of communications signals," *IEEE Trans. Microw. Theory Tech.*, vol. 53, no. 6, pp. 2179–2186, Jun. 2005.